

MHD CASSON FLUID STAGNATION POINT FLOW AND HEAT TRANSFER OVER AN EXPONENTIALLY STRETCHING SURFACE IN PRESENCE OF UNIFORM HEAT SOURCE AND SINK WITH SUCTION EFFECT

B. LAKSHMI¹, G.V. PRADEEP², C.B. MOHAN³

Manuscript received: 15.02.2022; Accepted paper: 18.09.2022;

Published online: 30.09.2022.

Abstract. The present study reveals the analysis of steady mixed convection MHD stagnation point flow of Casson fluid of non-Newtonian nature and Heat transfer over an exponentially stretching surface where the consequence of uniform heat source and sink are taken in to consideration. The presiding Non-linear Partial differential equations and the corresponding boundary conditions are formulated and thus transformed into pair of non-linear ordinary differential equations. The equations thus obtained are deciphered using Runge-Kutta fourth - order method with the help of MATLAB software. The results obtained for Skin friction coefficient and heat transfer rate for the case of Newtonian fluid are determined, which are in good harmony with the previously proclaimed results of other researchers. The impact of physical quantities such as Casson parameter, buoyancy parameter, Hartmann number, Prandtl number, heat source and sink, Suction parameter, on the fluid velocity and temperature are discussed through graphs for both assisting and opposing flow. The variation in Skin friction coefficient and Nusselt number are tabulated for various values of Hartmann number. Divergence in the velocity profile is observed for increase in Suction for two different values of Velocity ratio parameter. As Skin friction coefficient escalates with suction parameter indicating the exertion of drag force by the surface on the fluid flow. Also, the study reveals that the impact of Hartmann number is to minimize the boundary layer separation.

Keywords: Magneto hydrodynamics; Hartmann number; assisting and opposing flow; non-Newtonian; two-fold solution.

1. INTRODUCTION

A comprehensive investigation was performed by many analysts on the magnetohydrodynamic boundary layer flow and heat transfer due to exponential stretching as it plays an essential role in catalytic reaction, blood plasma phoresies devices etc. The reflex of considering thermal radiation on MHD flow over an exponentially stretching surface was studied by Bidan and Nadeem [1]. The work was further extended by Ishak [2] where the

¹ Prayoga Institute of Educational Research, Department of Mathematics, Bengaluru, 560082 Karnataka, India. E-mail: lakshmi.pradeep@prayoga.org.in.

² Visvesvaraya Technological University, Department of Mechanical Engineering, Belagavi, 590018 Karnataka, India. E-mail: pradeepgv78@gmail.com.

³ Centre for Incubation, Innovation, Research and Consultancy, Department of Mechanical Engineering, Bengaluru, Karnataka, India. E-mail: Mohan.cb@ciirc.jyothyit.ac.in.

radiation effect and magnetic effects are contemplated and analyzed the measure of heat transfer at the boundary surface with variation in magnetic parameter, radiation effect.

Further considering many physical parameters Mukhopadhyay et al. [3] studied the partial slip effect with a permeable sheet. According to Ali [4] there exist a dual solution for the opposing flow for the stagnation point flow due to vertical stretching with external magnetic field. Suction/blowing effect on casson fluid flow and heat transfer due to exponentially stretching porous surface with thermal radiation was analysed by Pramanik [5]. The study revealed that rise in the casson parameter has a drastic impact on the thickness of the temperature and velocity boundary layer. Later Siddheshwar [6] examined the causatum of varies non-dimensional numbers on the velocity and temperature profile by considering electrically conducting newtonian fluid. The occurrence of dual solution for shrinking sheet was indicated in the journal by Subhashini et al. [7] in the study of nanofluid flow due to exponentially stretching/shrinking sheet. The study on stagnation point flow was also accomplished by Shen et al. [8] by considering vertically stretching surface where the sheet is stretched nonlinearly in presence of suction, buoyancy parameter and slip effect and the study was able to conclude that the temperature inside the boundary layer drops with rise in suction and buoyancy parameter.

A mathematical model was developed by Hussain et al. [9] on casson nano-fluid flow by considering viscous dissipation and convective boundary conditions was able to find both thermal and nanoparticle concentration boundary layer thickness are higher for the larger values of thermophoresis parameter. Hafidzuddin et al. [10] considered exponentially stretching permeable sheet with generalizes slip effect was competent to carry out stability analysis of the solution and found that upper branch solution is stable compared to lower branch solution. Heat and mass transfer analysis was conducted by Raju et al. [11] with a magneto hydrodynamic casson fluid over an exponentially stretching permeable surface. Hayat et al. [12] investigated the MHD nonlinear convective flow of walters-b nano fluid of variable thickness with nonlinear stretching. Further Mahboob [13] studied MHD stagnation point flow and heat transfer of a nano fluid over a stretching surface with a homotopy analysis. The MHD stagnation point flow and heat transfer of a nano fluid with melting was studied by Wubshet [14]. The magneto hydro dynamic Jeffery nano-fluid flow with joule heating and viscous dissipation was analyzed by Shazad [15] and found that the silver-water nano fluid has comparatively less velocity, than those of the base fluid. numerical and graphical investigation was carried out on the MHD casson fluid flow and heat transfer due to stretching sheet in presence of suction and blowing by Lakshmi et al. [16].

An extensive study was conducted on the MHD stagnation point flow due to a vertical stretching sheet by Sharma et al. [17] in view of external magnetic field. where many physical parameters are introduced in order to study their jolt on velocity and temperature field. The work was extensive on the study of existence of dual solution for assisting and opposing flow. The MHD stagnation-point flow over an exponentially stretching/shrinking sheet with suction/injection, velocity slip effects were presented by Jamaluddin et al. [18]. The study concluded that when the values of suction parameter, magnetic and velocity slip parameters are rised, the range of the no uniqueness of the solution also increases.

Kumar et al. [19] considered electrically conducting casson fluid flow over an exponentially stretching curved sheet with thermal radiation effect. Lund [20] presented an investigation on stagnation point flow of casson fluid for shrinking /stretching sheet wherein also performed stability analysis with thermal radiation and viscous dissipation effects. The study was able to detect a dual similarity solution to the flow problem. The non-similar solutions of MHD mixed convection over an exponentially stretching surface with influence of non-uniform heat source or sink was studied by Patil et al. [21]. The study was also able to detect the fact that increase in prandtl number has an urge of reducing the width of thermal

boundary layer. The study was conducted numerically and graphically using various physical parameters on the velocity, temperature, wall transfer rate.

The present study aims at the investigation of Magneto hydrodynamic steady Casson fluid stagnation point flow and heat transfer that with Suction effect in presence of uniform source and sink. The impact of variation in the values of different parameters like Prandtl number, heat source/sink, velocity ratio parameters, buoyancy parameter, Hartmann number on the fluid flow and heat transfer are analyzed through graphs. The effect of variation in Casson parameter on the velocity, thermal boundary layer thickness is studied by for both assisting and opposing flow. Variation in skin friction coefficient and Nusselt number are noticed for various values of physical parameters through graphs.

2. PROBLEM FORMULATION

Mathematical formulation is accomplished by considering the steady flow to be along the stretching sheet positioned along x-direction such that y-axis is perpendicular to it. The stretching velocity is denoted by

$$u = u_{\text{exp}}(x) = ae^{x/L}$$

and

$$u = u_s(x) = be^{x/L}$$

is the free stream velocity. Where u and v be velocity components in x and y directions.

The rheological equation of state for an isotropic and incompressible flow of a Casson fluid is taken as

$$\tau_{ij} = \begin{cases} 2 \left(\mu_B + \frac{p_y}{\sqrt{2\pi}} \right) e_{ij}, \pi > \pi_c \\ 2 \left(\mu_B + \frac{p_y}{\sqrt{2\pi}} \right) e_{ij}, \pi < \pi_c \end{cases} \quad (1)$$

where $\pi = e_{ij}e_{ij}$ and e_{ij} denotes the $(i,j)^{th}$ component of the deformation rate, π the produce of the component of deformation rate with itself, π_c , a critical value and μ_β is plastic dynamic viscosity of the non-Newtonian model.

Let us know consider the equations associated with the given problem as Continuity equation, Momentum equation, Energy equations these can be represented mathematically as follows:

Continuity equation

$$\frac{\partial u}{\partial x} + \frac{\partial v}{\partial y} = 0 \quad (2)$$

Momentum equation

$$u \frac{\partial u}{\partial x} + v \frac{\partial u}{\partial y} = \nu \left(1 + \frac{1}{\beta} \right) \frac{\partial^2 u}{\partial y^2} + u_e \frac{du_e}{dx} - \frac{\sigma H_0^2 \mu_e^2}{\rho} (u - u_e) + g\beta(T - T_\infty) \quad (3)$$

Energy equation

$$u \frac{\partial T}{\partial x} + v \frac{\partial T}{\partial y} = \frac{K}{\rho c_p} \frac{\partial^2 T}{\partial y^2} + \frac{Q}{\rho c_p} (T - T_\infty) \quad (4)$$

2.1. BOUNDARY CONDITIONS

Let the boundary conditions defined for the problem are as follows,

$$\text{At } y = 0, v = V(x) = V_0 e^{\frac{x}{2L}}, u = u_{exp} = b e^{\frac{x}{L}}, T = T_w(x) = T_\infty + T_0 e^{x/2L} \quad (a)$$

$$\text{As } y \rightarrow \infty, u = u_s(x) = a e^{\frac{x}{L}}, T = T_\infty \quad (b)$$

where,

$u = u_s(x) = a e^{\frac{x}{L}}$ is the free stream velocity

$u = u_{exp}(x) = b e^{\frac{x}{L}}$ Stretching velocity

$T_w = T_\infty + T_0 e^{x/2L}$ is the temperature at the sheet

T_0 = the reference temperature

$V(x) = V_0 e^{\frac{x}{2L}}$ is the velocity of the fluid at the wall, if $V(x)$ greater than zero then it represents the velocity of suction that is $V(x) > 0 = S$.

3. METHOD OF SOLUTION

In order to solve equations (3) and (4) the following similarity transformations are used since they are non-linear in nature and also on the boundary conditions represented by (a),(b) to convene in to simplest form,

$$\eta = \sqrt{\frac{a}{2vL}} e^{x/2L} y \quad (5)$$

$$\psi = \sqrt{2avL} e^{x/2L} f(\eta) \quad (6)$$

$$u = a e^{x/L} f'(\eta) \quad (7)$$

$$v = -\sqrt{\frac{va}{2L}} e^{x/2L} [f(\eta) + \eta f'(\eta)] \quad (8)$$

$$T = T_\infty + (T_w - T_\infty) e^{x/2L} \theta(\eta) \quad (9)$$

The modified momentum and energy equations are,

$$\left(1 + \frac{1}{\beta}\right) f'''(\eta) + f(\eta)f''(\eta) - 2(f'(\eta))^2 - 2H_a^2 e^{-X}(f'(\eta) - 1) + 2\lambda\theta(\eta) + 2 = 0 \quad (10)$$

$$\theta''(\eta) - P_r[f'(\eta)\theta(\eta) - f(\eta)\theta'(\eta)] + 2P_r\delta e^{-X} = 0 \quad (11)$$

The boundary conditions (a) and (b) takes the form: at $\eta = 0$, $f'(\eta) = \frac{be^{\frac{x}{L}}}{ae^{\frac{x}{L}}} = b/a = A$, $f(0) = S$, $\theta = 1$ and as $\eta \rightarrow \infty$, $f' = 1$, $\theta = 0$.

The Skin friction coefficient is defined as:

$$C_f(\text{Re}_x)^{1/2} \sqrt{\frac{2l}{x}} = \left(1 + \frac{1}{\beta}\right) f''(0).$$

The Nusselt number is defined as:

$$Nu_x = \frac{xq_w}{k(T_w - T_\infty)} = -(\text{Re}_x)^{-1/2} f(\infty) \theta'(0)$$

The following substitutions are considered in order to reduce the equations (10) and (11) into simple first order differential equations

$$\begin{aligned} f &= f_1, f' = f_2, f'' = f_3, f''' = f'_3, \theta = f_4 \\ \theta' &= f_5, \theta'' = f'_5 \end{aligned} \quad (12)$$

Therefore, the equation (10) and (11) takes the form

$$f'_1 = f_2, f'_2 = f_3$$

$$f'_3 = \frac{1}{\left(1 + \frac{1}{\beta}\right)} [2f_2^2 - f_1f_3 + 2H_a^2 e^{-X}(f_2 - 1) - 2\lambda f_4 - 2] \quad (13)$$

$$f'_5 = P_r(f_2f_4 - f_1f_5) - 2P_r\delta e^{-X}f_4 \quad (14)$$

Transformed boundary conditions are,

$$f_1(0) = 0, f_2(0) = A, f_3(0) = f'_3(0) = S, f_4(0) = 1,$$

$$f_3(\infty) = 1, f_4(\infty) = 0.$$

4. RESULTS AND DISCUSSIONS

The equations (13) and (14) are the first order ordinary differential equations with the transformed boundary conditions which are thus solved using fourth order Runge-Kutta method and the numerical calculations followed by graphs are drawn with aid of BVP47 using MATLAB software.

The following Tables 1 and 2 gives the agreement of the present results with the previously published results of obtained for Skin friction coefficient $f''(0)$ for various values of Casson parameter β and Nusselt number for various values of Prandtl number Pr .

Table1. The value $f''(0)$ is calculated for Newtonian Casson fluid flow $\beta=0$.

Values of the parameter	A. Jamaludin [17]	Subhashini S V [7]	Present study
$H_a = X = \mu \delta = \lambda = 0$	1.6872	1.6863	1.6871

Table 2. Calculation of Nusselt number for various values of $H_a=0$, $X=0$, $S=0$, $\delta=0$, $\lambda=0$ with variation in Prandtl number (P_r).

P_r	Bidan and Nazar[1]	Ishak [2]	Present work
1	0.9547	0.9548	0.9548
3	1.8691	1.8691	1.8691
5	2.5001	-	2.5000

Table 3. The calculation of $f''(0)$ and Nusselt number $-\theta'(0)$ with variation in Ha with $A=0.5$, $Pr=0.7$, $S=\beta=\delta=0$.

Ha	Assisting flow $\lambda=0.5$		Opposing flow $\lambda=-0.5$	
	$f''(0)$	$-\theta'(0)$	$f''(0)$	$-\theta'(0)$
0	1.7112	0.9785	-0.3452	0.7991
1	1.7854	0.9874	0.0876	0.8796
3	1.9897	0.9923	0.7121	0.8976
5	3.2023	1.0001	2.967	0.9673
10	5.9878	1.2463	5.001	1.0012

Table 4. The calculation of $f''(0)$ and $-\theta'(0)$ with respect to variation in Ha with $A=1$, $Pr=0.7$, $S=\beta=\delta=0$.

Ha	Assisting flow $\lambda=0.5$		Opposing flow $\lambda=-0.5$	
	$f''(0)$	$-\theta'(0)$	$f''(0)$	$-\theta'(0)$
0	-1.3765	1.4543	-2.7623	1.3421
1	-1.8823	1.3987	-2.8123	1.2543
3	-2.675	1.2231	-3.5672	1.1213
5	-5.453	1.1987	-5.984	1.0342
10	-9.9978	1.1123	-10.564	1.0001

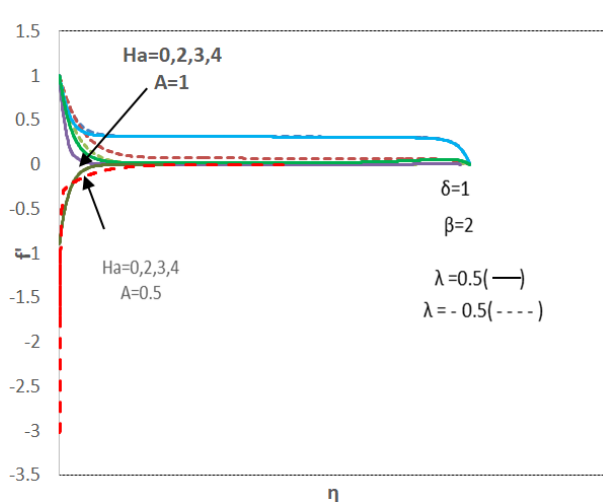


Figure 1. Velocity profile for Ha with $S=0.5$, $Pr=0.7$.

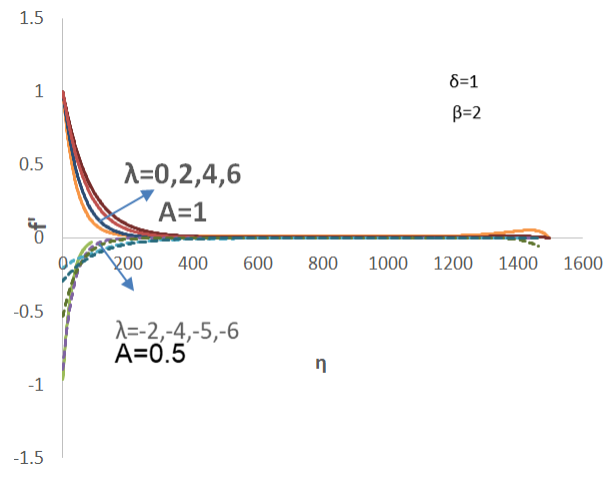


Figure 2. Velocity profile for buoyancy parameter with $S=0.5$, $Pr=0.7$.

The Fig. 1 exhibits two-fold solution on account of increase in Hartmann number Ha on the velocity profile $f'(\eta)$ for a fixed values of $\beta=2$, $\delta=1$, $Pr=0.7$ which includes both assisting flow (for $\lambda=0.5$) and opposing flow (for $\lambda=-0.5$). As the value of Ha increases for small rise in the velocity ratio parameter $A=0.5$ to $A=1$ more and more fluid will be rushed towards the boundary surface so the flow will be retarded at some particular point. This correlates the depletion of $f'(\eta)$. Which also minimizes the boundary layer separation.

The above Fig. 2 represents escalation in $f'(\eta)$ with rise in buoyancy parameter λ , this could be noticed more predominant for $\lambda>0$ and $A=1$. This is because as λ increases, the kinetic energy of the fluid particle also increases which accelerates the flow rate. This could be the indication of two-fold solution, this is clearly reflected in the above Fig. 2 for $A=0.5$.

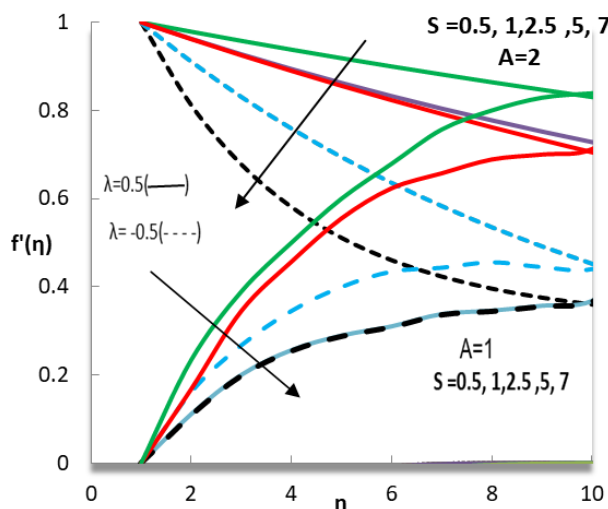


Figure 3. Velocity profile for Suction parameter S with $Pr=0.7$, $\beta=2$, $Ha=\delta=1$

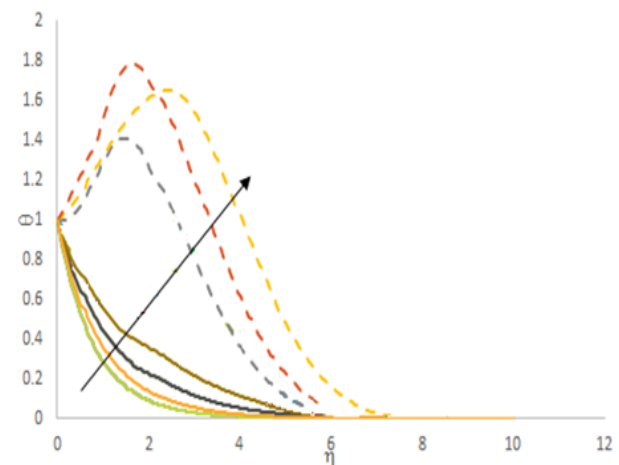


Figure 4. Temperature profile for $\lambda = -2, -3, -4, 0, 2, 3$, with $\beta=2$, $\delta=1$, $S=0.5$, $A=Ha=1$.

The $f'(\eta)$ diverges from a point and drops for increase in suction parameter for $A=1$ and for $A=2$ associated with both $\lambda>0$ and $\lambda<0$. The fluid velocity declines gradually, this suppress in velocity field is more presiding at $\lambda=-0.5$. This results in the decrease in the boundary layer width. This intern helps in the loss of energy by preventing the boundary layer detachment by decreasing the frictional losses.

It can be noticed from the Fig. 4 that for the opposing flow of $\lambda = -2, -3, -4$ the graph shoots up drastically which implies that the temperature inside the boundary layer increases with rise in λ with $A=1$ but there is reduction in the temperature field for $\lambda=0, 2, 3$.

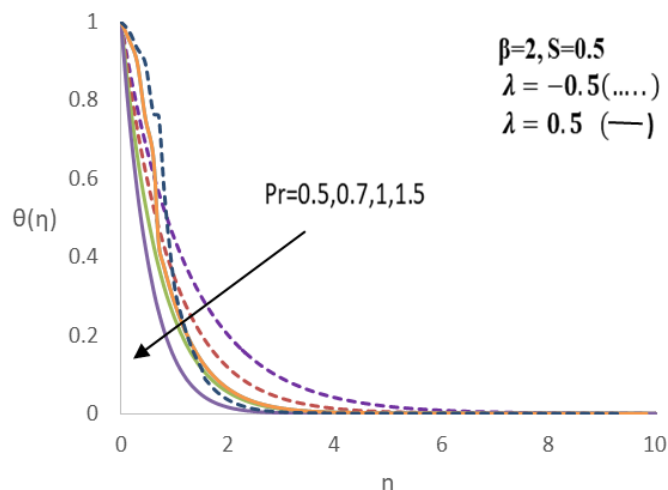


Figure 5. Temperature profile for Pr with data $Ha=1$, $\beta=2$, $S=0.5$, $Pr=\delta=A=1$.

As Pr increases, $\theta(\eta)$ drops. This also leads to the thinning of thermal boundary layer because with rise in, thermal diffusivity decreases this correlates the energy transfer rate which leads to the thinning of thermal boundary layer. This Phenomenon is more predominant when $\lambda > 0$.

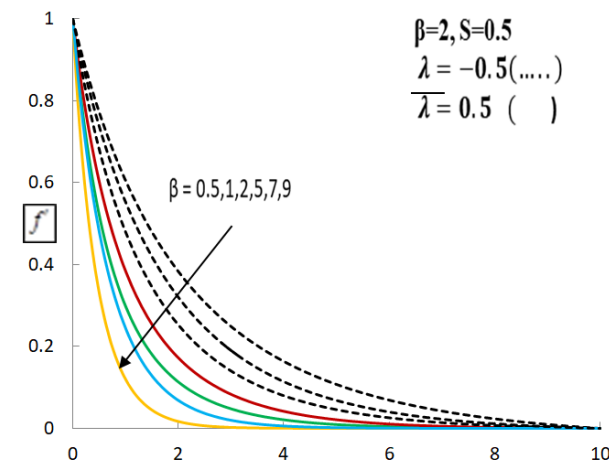


Figure 6. Velocity profile for β with the data $\delta = A = Ha = 1, S = 0.5, Pr = 0.7$.

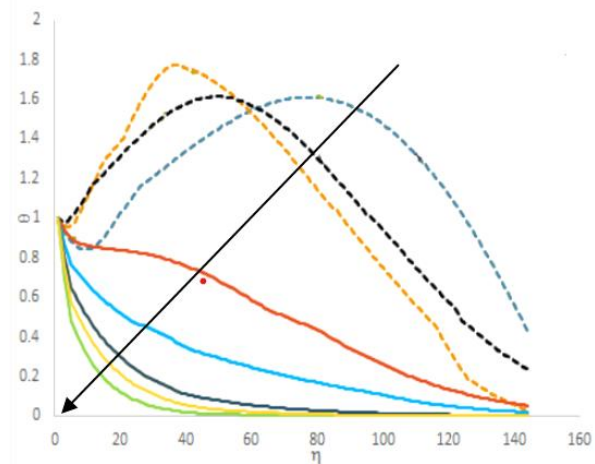


Figure 7. Temperature profile for $\beta = 1.5, 3, 5.5, 10, 12, 13$ with $Ha = Pr = \delta = a = 1, S = 0.5$ for $\lambda = 0.5, \bar{\lambda} = -0.5$.

Fig. 6 represents the velocity profile for increase in the β for $\lambda < 0$ and for $\lambda > 0$. The $f'(\eta)$ drops resulting in the declination of velocity boundary layer thickness this is because of the resistance created to the flow by the increase in the β and as the value increases to infinity the fluid almost behaves like a Newtonian fluid. The Fig. 7 establishes the relation between the variations in $\theta(\eta)$ with respect to the β . It has been noticed that for the $\theta(\eta)$ shoots up for $\lambda < 0$ but for $\lambda > 0$ that is for assisting flow the temperature drops with respect to increase in the value of β in presence of suction. It is clearly observed from the above Fig. 8 that the $\theta(\eta)$ decreases with increase in the value of A . The effect is noticed in both the $\lambda < 0$ and for $\lambda < 0$. Figs. 9 and 10 show rise in $f'(\eta)$ with increase in δ also it can be easily detected that the temperature of the fluid inside the boundary layer rises as the parameter δ increases. The effect is more dominant in case of $\delta > 0$ that for heat source. As a result of this it is obvious to say that the thermal boundary layer thickness decreases or shrinks a bit for $\delta < 0$ but increases rapidly for the case of heat source $\delta > 0$.

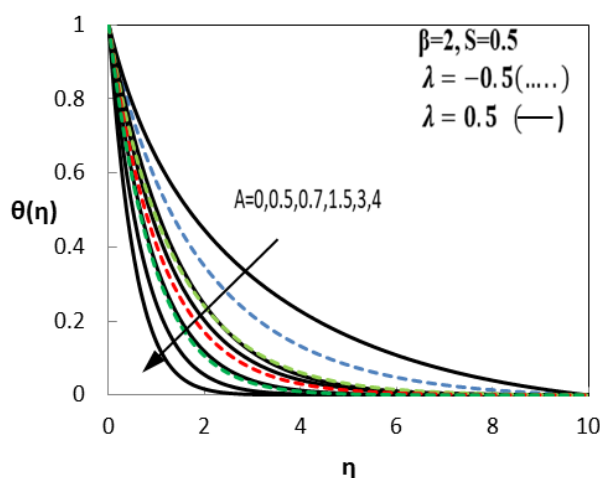


Figure 8. Temperature profile for Velocity ratio parameter A , with $\delta = Ha = 1$.

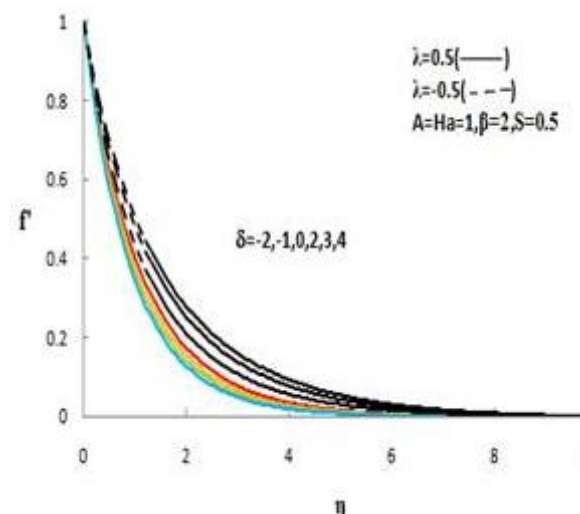


Figure 9. Velocity profile for different values of heat source and sink parameter.

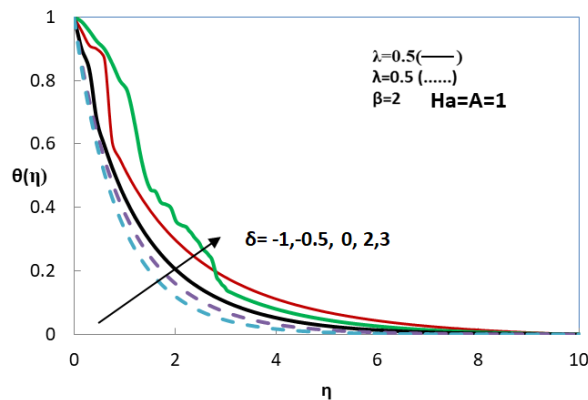


Figure 10. Temperature profile for different values of heat source and sink.

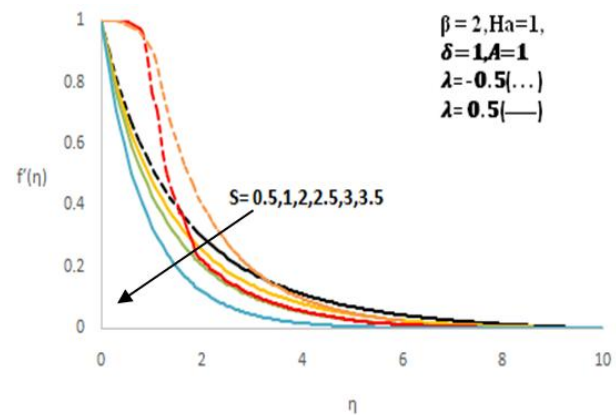


Figure 11. Velocity profile for different values of Suction parameter.

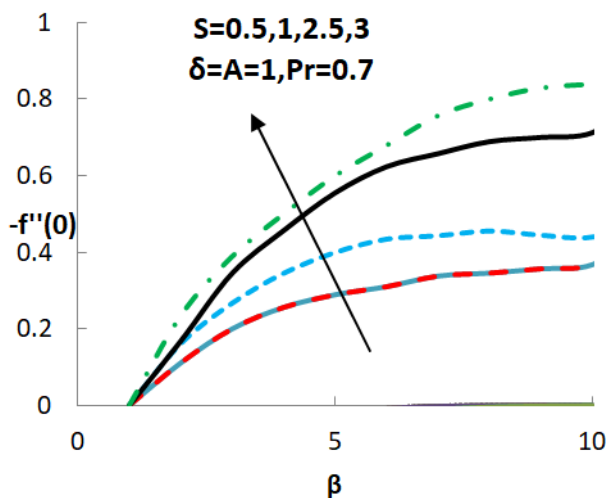


Figure 12. Variation in $-f''(0)$ with β .

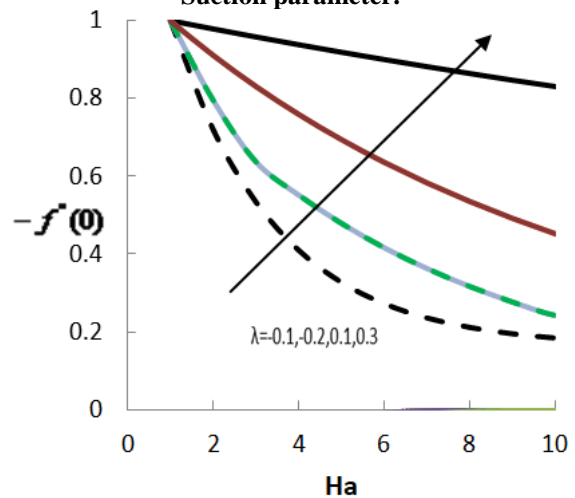


Figure 13. Variation in $-f''(0)$ with Ha for both assisting and opposing flow $\delta=A=1$, $Pr=0.7$, $S=0.5$.

Fig. 11 shows that $-f''(0)$ increases with Suction indicating the drag force that is exerted by surface on the fluid. It is evident from Fig. 13 that the $-f''(0)$ increases with Ha for $\lambda < 0$ but the effect is more rapid for $\lambda > 0$.

5. CONCLUSIONS

As the value of Ha increases for small increase in the velocity ratio parameter $A=0.5$ to $A=1$, more and more fluid will be rushed towards the boundary surface so the flow will be retarded at some particular point. This results in the depletion of the velocity profile. The Velocity accelerates with rise in λ this could be noticed more predominant in the case of assisting flow and velocity ratio parameter $A=1$. The fluid velocity decreases gradually but this suppress in velocity field is more presiding at $\lambda < 0$. The temperature profile shoots up for $\lambda < 0$ but for $\lambda > 0$ temperature drops with respect to increase in β with S . The velocity of the fluid drops resulting in the declination of velocity boundary layer thickness for increase in the $-f''(0)$ for both $\lambda > 0$ and $\lambda < 0$. The temperature of the fluid increases as the parameter δ increases. The effect is more dominant for $\delta > 0$ that for heat source. It is found that as $-f''(0)$ escalates with S indicating the drag force is exerted by the stretching surface on the fluid. The $-f''(0)$ increases with Ha for $\lambda < 0$ but the effect is more rapid for $\lambda > 0$.

REFERENCES

- [1] Nadeem, S., Zaheer, S., Fang, T., *Numerical Algorithms*, **57**, 187205, 2011.
- [2] Ishak, A., *Sains Malaysiana*, **40**, 391, 2011.
- [3] Mukhopadhyay, S., Gorla, R.S.R., *Heat and Mass Transfer*, **48**, 1773, 2012.
- [4] Ali, F., Nazar, R., Arifin, N., Pop, I., *Boundary Value Problems*, **2013**(1), 32, 2013.
- [5] Pramanik, S., *Ain Shams Engineering Journal*, **5**(1), 205, 2014
- [6] Siddeshwar, P.G., *Journal of applied fluid mechanics*, **7**(2), 367, 2014.
- [7] Subhashini, S.V., Sumathi, R., Momoniat, E., *Meccanica*, **49**, 2467, 2014.
- [8] Shen, M., Chen, H., *Boundary Value Problems*, **2015**, 78, 2015.
- [9] Hussain, T., Shehzad, S.A., Alsaedi, A., Hayat, T., Ramzan, M., *Journal of Central South University*, **22**, 1132, 2015.
- [10] Hafidzuddin, E.H., *Journal of Applied Fluid Mechanics*, **9**(4), 2025, 2016.
- [11] Raju, C.S.K., Sandeep, N., *Engineering Science and Technology - An International Journal*, **19**(1), 45, 2016.
- [12] Hayat, T., *International Journal of Heat and Mass Transfer*, **110**, 506, 2017.
- [13] Mabood, F., Khan, W.A., Ismail, A.I.M., *Journal of King Saud University - Engineering Sciences*, **29**, 68, 2017.
- [14] Wubshet, I., *Propulsion and Power Research*, **6**(3), 214, 2017.
- [15] Shahzada, F., Sagheer, M., Hussain, S., *AIP Advances*, **8**, 065316, 2018.
- [16] Lakshmi, B., Pradeep, G.V., *International Journal of Mechanical Engineering and Technology*, **7**(5), 18, 2016.
- [17] Sharma, P.R., Sinha, S., Yadav, R.S., Filippov, A.N., *International Journal of Heat and Mass Transfer*, **117**, 780, 2018.
- [18] Jamaludin, A., Nazar, R., Pop, I., *Journal of Physics: Conference Series*, **1366**, 012040, 2019.
- [19] Ananth Kumar, K., Sugunamma, V., Sandeep, N., *Journal of Thermal Analysis and Calorimetry*, **140**, 5, 2020.
- [20] Lund, L.A., *Scientific Reports*, **10**, 15405, 2020.
- [21] Patil, P.M., Latha, D.N., Chamaka, A.J., *Journal of Applied and Computational Mechanics*, **2021**, 1334, 2021.